SPACE TELESCOPE SCIENCE INSTITUTE
Operated for NASA by AURA

Instrument Science Report WFC3 2006-01

Results of WFC3 Thermal Vacuum Testing: IR Channel Subarray Photometry

B. Hilbert
May 18, 2006

ABSTRACT

The photometric accuracy of WFC3's IR Channel was examined during thermal vacuum testing in September - October, 2004. The measured signal levels from various incident flux levels and sample sequences were compared in order to determine the relative accuracy of FPA64. Significant deviations in measured versus expected flux levels were observed at some illumination levels.

Introduction

The purpose of this SMS, performed during the September - October 2004 thermal vacuum testing campaign, was to test the photometric accuracy of WFC3's IR channel over a range of incident fluxes. By imaging point sources with various known fluxes, and comparing the detected signals to the real fluxes, we were able to test the relative accuracy of FPA64.

Data

The data used for this analysis were part of the IR22 test. These files were composed of RAPID and SPARS10 ramps of various lengths. Details are presented in Table 1. All ramps were taken at the nominal gain value of 2.5 e^-/ADU.

At each of 5 Optical Stimulus (OS) flux levels, a series of 4 point source ramps were taken, followed by a set of dark current ramps. At the end of the test, a pair of point source

files were taken at a 6th OS flux level. For each set of 4 point source ramps, the illuminating fiber was moved between each file, such that the point source fell in a different quadrant in each ramp.

The penultimate set of point sources, with incident flux values of 5,179,000 photons/sec, displayed saturated pixels in all reads of the ramp files. Without an accurate measurement of the detected flux, these files were not useful for examining the photometric accuracy of FPA64, and were ignored. Similarly, the point sources in ramps 27 and 28 displayed saturated pixels in the final read of the ramps, leaving only two reads with good signal measurements. This translated into a single good measurement of flux rates for each ramp, limiting the accuracy of subsequent data analysis.

Ramp Number	Sample Sequence	Array Size (pixels)	# Reads per Ramp	Exposure Time (sec)	Total Flux (Photons/sec)	Point Source or Dark	# of Files
0	RAPID	1024	15	67.0	NA	Dark	1
1-5	RAPID	64	15	0.9	NA	Dark	5
6-10	SPARS10	64	15	78.7	NA	Dark	5
11-14	SPARS10	64	15	78.7	11,146*	Point Source	4
15	RAPID	1024	15	67.0	NA	Dark	1
16-20	RAPID	64	15	0.9	NA	Dark	5
21-25	SPARS10	64	15	78.7	NA	Dark	5
26-29	SPARS10	64	3	11.3	83,691	Point Source	4
30	RAPID	1024	15	67.0	NA	Dark	1
31-35	RAPID	64	15	0.9	NA	Dark	5
36-40	SPARS10	64	15	78.7	NA	Dark	5
41-44	RAPID	64	15	0.9	88,864	Point Source	4
45	RAPID	1024	15	67.0	NA	Dark	1
46-50	RAPID	64	15	0.9	NA	Dark	5
51-55	SPARS10	64	15	78.7	NA	Dark	5
56-59	RAPID	64	15	0.9	766,460	Point Source	4
60	RAPID	1024	15	67.0	NA	Dark	1
61-65	RAPID	64	15	0.9	NA	Dark	5
66-70	SPARS10	64	15	78.7	NA	Dark	5
71-74	RAPID	64	8	0.485	5,179,800	Point Source	4
75	RAPID	1024	15	67.0	NA	Dark	1
76-80	RAPID	64	15	0.9	NA	Dark	5

Ramp Number	Sample Sequence	Array Size (pixels)	# Reads per Ramp	Exposure Time (sec)	Total Flux (Photons/sec)	Point Source or Dark	# of Files
81-85	SPARS10	64	15	78.7	NA	Dark	5
86	SPARS10	64	15	78.7	10,830	Point Source	1
87	RAPID	1024	15	67.0	10,830	Point Source	1

Table 1. Data files in the IR22 test, used to check the photometric accuracy of the IR channel. Flux values give the total flux from the Optical Stimulus (OS), and were obtained from the header of each file. * - The 11,146 photons/sec OS flux value was not present in the data headers, and was calculated by Randal Telfer (priv. communication), and is estimated to have an uncertainty comparable to the other OS flux values, of a few percent.

Analysis

Data ramps were first run through the IR data reduction pipeline, in order to perform basic data reduction steps (Hilbert, 2004), including the non-linearity correction described by Robberto and Hilbert (2005). The outputs from the pipeline included a masked ramp, as well as a final image, in units of electrons per second, for each ramp. A flat field image from a previous thermal vacuum test was used to remove spatial variations in sensitivity from the ramps. Prior to the application of the flat field image, the point sources located in quadrant 3 were affected by a dust feature on the CSM. This dust feature reduced the observed flux in these point sources by ~20% - 30%. After applying the F105W flat field image to all ramps, the effects of the dust feature were minimized. This can be seen in Figure 3, where the fluxes detected in all quadrants are roughly equal. After these initial processing steps, photometry was performed on the point sources in these ramps and final images.

Aperture photometry was performed on sources in each read of each ramp. Aperture radius was dictated by the maximum distance from the center of the source at which pixels' signals were at least 5σ above the mean local background level. Background subtraction was performed, but had a negligible effect on the photometry, due to the small (< 1 e^-/pixel/sec) signal falling on FPA64 outside the region of the point source. The photometry results for all files are shown in Figure 1, where the ramps taken at each of six different OS flux levels are obvious.

Photometry results for each group of 4 point source images (as seen in Table 1) were averaged together, to create a mean measured flux rate for each incident flux. Table 2 reports these measured mean fluxes, along with their values relative to the mean flux from the ramps with the highest signal point sources. These photometry results, along with photometry of individual reads, were used to check the photometric accuracy of the IR channel.

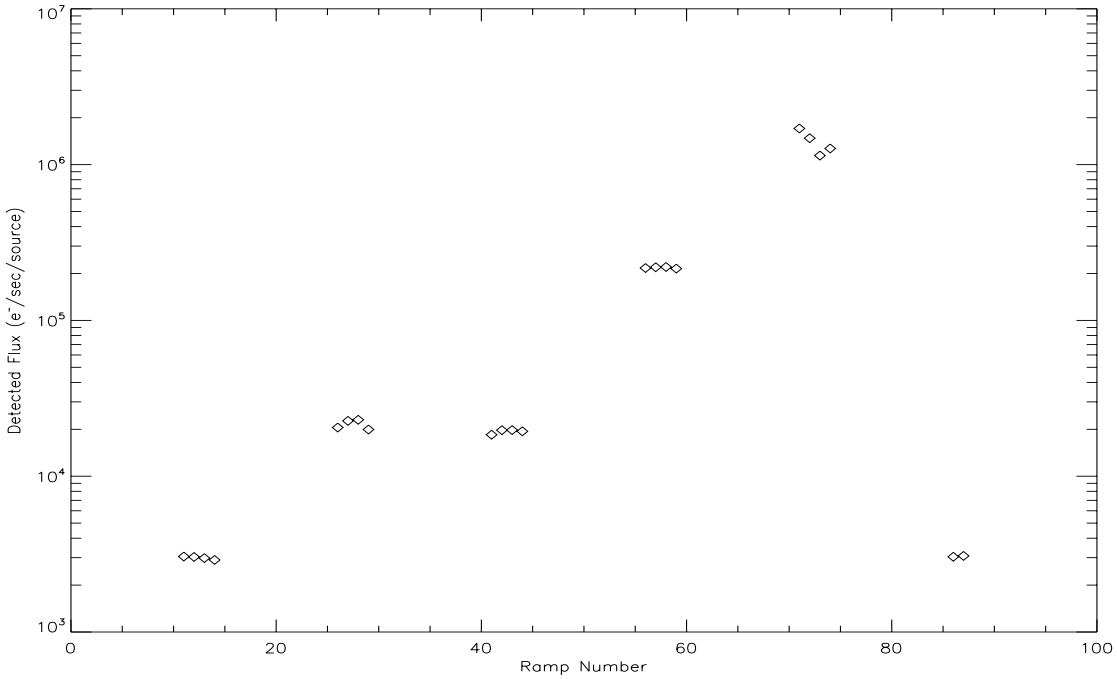

Figure 1: Photometry results for point source files listed in Table 1. The point sources represented by the group of files with the highest signal (ramps 71 - 74) contained saturated pixels beginning in the first read, and were ignored. Flux levels for ramps 27 and 28 are based on a single flux measurement, as only 2 reads in each ramp were free from saturated pixels.

Flux Ratios

By comparing the flux ratios from the photometry of the final images to similar flux ratios derived from the reported incident Optical Stimulus (OS) fluxes, the relative photometric accuracy of FPA64 at various flux levels was examined.

As seen in Table 2, each observed flux ratio was lower than the corresponding OS flux ratio. The observed flux ratios ranged from 0.5 to 8.9σ below the expected ratios. This suggests that FPA64 detected too little flux from the dimmer point sources, relative to the brightest point source. Unfortunately, with a maximum of only 4 ramps at each flux level, the uncertainties in the means listed in Table 2 may suffer from small-number statistics. This is especially true in the case of the second group of point sources. Saturated pixels in the final reads of ramps 27 and 28 forced a calculation of the source flux from only 2 reads (i.e. a single signal difference). Nevertheless, the mean measured flux values appear to be systematically low.

Figure 2 shows the measured flux values separated by quadrant. The quadrant numbering convention followed here matches that used in other thermal vacuum data analyses, with quadrant 1 in the lower left, and quadrant numbers increasing in a clockwise direction. For each of the first 4 groups of point sources, the measured flux values in each quadrant were normalized by the mean measured flux, and plotted. The resulting plot shows that for most incident flux rates, quadrants 1 and 2 measured fluxes below average, while fluxes in quadrants 3 and 4 were above average, where the average values deviate from the expected values by 5% - 23%.

Measured Mean Flux (e^-/sec)	**Uncertainty in Mean Flux (e^-/sec)**	**Ratio Relative to Highest Flux Ramps**	**Uncertainty in Ratio (1σ)**	**Ratio from OS Fluxes**	**Measured VS Calculated Ratio Difference (σ)**
2,990	70	0.0137	0.0003	0.0145	2.7
21,500	1520	0.0986	0.0071	0.1092	1.5
19,400	620	0.0890	0.0030	0.1159	8.9
218,000	2,330	1	NA	1	NA
3,060	30	0.0140	0.0002	0.0141	0.50

Table 2. Measured versus reported fluxes and flux ratios for the point sources in the IR22 data. The worst-case has the measured OS flux ratio ~8.9σ from the measured flux ratio. Uncertainties in the mean flux values represent the standard deviation of the individual flux values that contributed to each mean flux value, and may therefore suffer from small-number statistics.

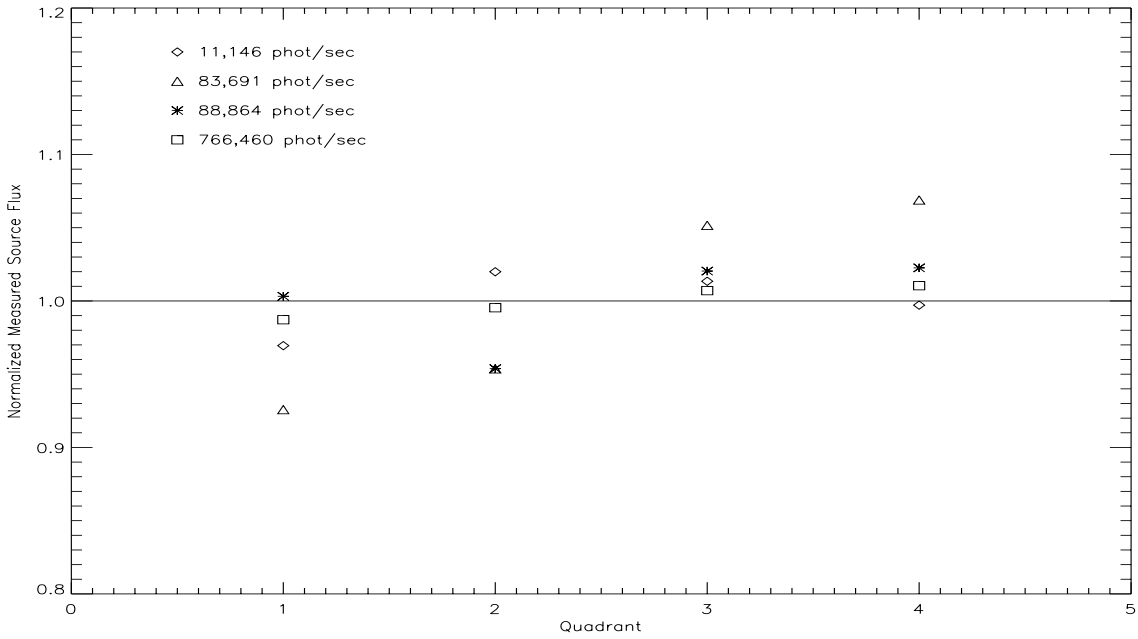

Figure 2: Quadrant-by-quadrant measured flux values for each of the first 4 groups of point sources. By normalizing each flux measurement versus its group mean, the behaviors of the quadrants relative to one another were examined. Quadrants 1 and 2 appear to detect consistently below average flux.

Ramp Non-linearity

In order to search for any residual non-linearity effects within the ramps, photometry, as described above, was also performed on the point source in each read of each ramp. The amount of flux measured between consecutive reads was examined for any variations. Examples of the flux rates are shown in Figure 3.

Any effects of charge trapping, as observed by Bohlin (2005) on NICMOS, should manifest themselves as increasing signal with time in the dimmest ramps. No nonlinearities of this kind are observed in these data, as seen in the bottom panel of Figure 3. More data with low-flux point sources are needed in order to better explore the presence or absence of charge trapping effects.

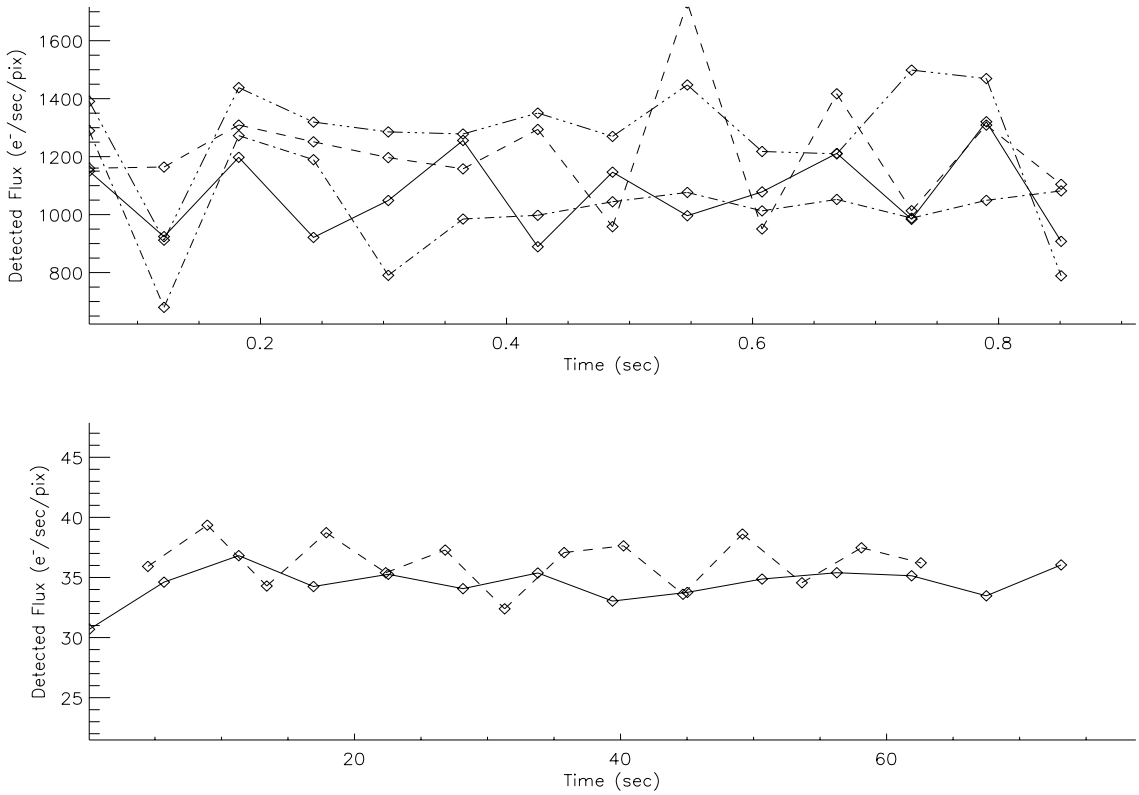

Figure 3: Point source flux up the ramp. Both plots show the signal rate measured in all ramps of a given flux. The top plot gives the detected flux in all four quadrants, at an incident flux rate of 88,864 photons/sec, while the bottom plot uses ramps with an incident flux of 10,830 photons/sec. The data used to produce the upper panel plot are also shown as the asterisks in Figure 2. The low signal level in quadrant 2 of Figure 2 corresponds to the dash-dot line in the upper panel here.

Conclusions

The observed low flux ratios seen in FPA64 imply that some mechanism is preventing FPA64 from measuring all the flux in the point sources for this test. The amount of "missing" flux does not appear to scale well with the intensity of incoming flux.

In addition, photometry of the reads within the data ramps shows a constant measured signal with time, implying that FPA64 is not affected by charge traps. Given this, there are two effects that could be contributing to the variations in the mean flux values and uncertainties. First, small number statistics could be skewing the results. Only a few ramps were taken at each flux level. Secondly, and possibly more importantly, untrackable variations in the CASTLE lamp flux probably had an effect on the results. Flux uncertainties were reported at the level of several percent. This is confirmed in the reported flux levels during the second and third set of point source ramps. The measured flux levels differ by 6% with no change in CASTLE setup. On the other hand, when CASTLE was stable, as it

appears to have been during the penultimate and final sets of pinhole ramps, the measured versus expected flux rates can be very close, even over a wide range of incident flux levels.

Recommendations

More point source data are needed in order to obtain robust values of the flux ratios and their uncertainties. This test is most sensitive to the effects of potential charge traps when the point source has a low incident flux and/or data ramps have short exposure times.

Data ramps such as those described within de Jong et al. (2006), aimed at exploring non-linearities related to charge trapping, should be collected.

Acknowledgements

Many thanks to Howard Bushouse and Massimo Robberto for lots of useful comments and insight on the analysis of these data.

References

Bohlin, R. C., Lindler, D. J., and Reiss, A., **Grism Sensitivities and Apparent Non-Linearities**. NICMOS Instrument Science Report 2005-02. http://www.stsci.edu/hst/nicmos/documents/isrs/isr_2005-02.pdf. May, 2005.

De Jong, R.S., Bergeron, E., Reiss, A., and Bohlin, R., **NICMOS Count-rate Dependent Non-linearity Tests using Flatfield Lamps**. NICMOS Instrument Science Report 2006-01. http://www.stsci.edu/hst/nicmos/documents/isrs/isr_2006-01.pdf. February, 2006.

Hilbert, B., **Basic IDL Data Reduction Algorithm for WFC3 IR and UVIS Channel**. WFC3 Instrument Science Report 2004-10. http://www.stsci.edu/hst/wfc3/documents/ISRs/WFC3-2004-10.pdf. June, 2004.

Robberto, M. and Hilbert B., **WFC3 2004 Thermal Vacuum Campaign: IR channel linearity (flat field illumination - SMS IR04)**. Instrument Science Report 2005-29. http://www.stsci.edu/hst/wfc3/documents/ISRs/WFC3-2005-29.pdf. December, 2005.